

NUMERICAL ANALYSIS OF PARASITIC CROSSING COMPENSATION WITH WIRES IN DAΦNE*

A. Valishev, FNAL, Batavia, IL 60510, USA, D. Shatilov, BINP, Novosibirsk, Russia
C. Milardi, M. Zobov, INFN/LNF, Frascati, Italy

Abstract

Current bearing wire compensators were successfully used in the 2005-2006 run of the DAΦNE collider to mitigate the detrimental effects of parasitic beam-beam interactions. A marked improvement of the positron beam lifetime was observed in machine operation with the KLOE detector. In view of the possible application of wire beam-beam compensators for the High Luminosity LHC upgrade, we revisit the DAΦNE experiments. We use an improved model of the accelerator with the goal to validate the modern simulation tools and provide valuable input for the LHC upgrade project.

INTRODUCTION

The long-range (also referred to as the parasitic) beam-beam interactions in colliders occur when the two particle beams moving in a common vacuum chamber and separated transversely, interact via the electromagnetic field. Such interactions may be a significant factor limiting the performance of multi-bunch particle colliders: for example, they were shown to impact the luminosity lifetime and increase particle losses during the Tevatron collider Run II [1]. At the Tevatron, the beams collided head-on in two high-luminosity Interaction regions (IR), and were separated by means of electrostatic separators in the rest of the machine, where each bunch experienced 70 parasitic interactions with the separation ranging from 6 to 10 of the beam σ . It was shown that four collisions at the smallest separation of 6σ were responsible for the dramatic degradation of lifetime of both beams [2]. At the LHC, the beams collide at an angle in the experimental IRs and move in separate vacuum chambers in the arcs. Still, the number of parasitic crossings in the common sections is up to 120 with 25 ns bunch spacing at the nominal transverse separation of 9.5σ [3]. Experiments during the LHC Run 1 have shown that with $\frac{1}{2}$ the nominal number of bunches (bunch spacing of 50 ns), the onset of high losses is at the transverse separation of $\approx 5\sigma$ for nominal bunch intensity [4]. The HL-LHC upgrade demands a two-fold increase in the total beam current [5], which leads to a significant enhancement of the long-range beam-beam effects [6]. As a consequence, the transverse separation of the two beams, and hence the crossing angle, has to be increased (to 12.5σ in the baseline scenario), which in turn leads to several undesired effects: the geometric loss of

luminosity, increased pile-up density, and the demand for large-aperture final focus magnets.

Compensator devices in the form of current-bearing wires (also referred to as the Beam-Beam Long-Range Compensators, BBLRC) were proposed as a way to mitigate the long-range beam-beam effects [7], and since were extensively studied both theoretically [8-10] and experimentally [11,12]. A remarkable demonstration of the effectiveness of BBLRC for improvement of collider performance was achieved during the 2005-2006 operation of DAΦNE at INFN/LNF (Frascati, Italy). The application of BBLRC devices during the KLOE run resulted in approximately 50% improvement of the average luminosity integration rate [13].

Numerical simulations of beam-beam effects with the weak-strong particle tracking code Lifetrac [14] guided the design of DAΦNE beam-beam compensation. Over the past decade, the code functionality has been considerably expanded. The most important additions include the implementation of Frequency Map Analysis (FMA) [15] and the ability to perform tracking in detailed machine lattices. The goals of the present work are to revisit the results of DAΦNE beam-beam compensation experiment using the modern computing tools, and demonstrate the predictive power of Lifetrac simulations with BBLRC for future applications.

EXPERIMENTAL DATA

We compiled a comprehensive set of machine and beam parameters during the 2005-2006 run with the KLOE detector (see Tab. 1). The collider performance data relevant to the BBLRC experiments is presented in Figs. 1, 2 showing the time dependence of electron and positron intensities, luminosity, and the beam-beam related portion of positron losses for the cases of BBLRC turned off and on, respectively. The beam-beam related loss rate \dot{N}_{BB} was derived from the total loss rate \dot{N} according to the following consideration:

$$\dot{N} = \dot{N}_{Lum} + \dot{N}_T + \dot{N}_{BB}$$

where $\dot{N}_{Lum} = \sigma_{tot}L$ is the luminous loss rate ($\sigma_{tot} = 0.048$ barn), \dot{N}_T is the Touschek loss rate, and the losses due to scattering on the residual gas are vanishingly small. The typical positron loss rate in the experimental runs was about 2×10^9 s⁻¹ (corresponding beam intensity lifetime $\tau \approx 10^3$ s), and was dominated by the Touschek and beam-beam effects with luminous losses being a relatively minor contribution at about 5×10^6 s⁻¹. The highlighted time intervals in Figs. 1, 2 are the data samples used for comparison with the beam-beam simulation as they represent stable beams in weak-strong

* Research supported by DOE via the US-LARP program and by EU FP7 HiLumi LHC - Grant Agreement 284404.

Content from this work may be used under the terms of the CC BY 3.0 licence (© 2015). Any distribution of this work must maintain attribution to the author(s), title of the work, publisher, and DOI.

mode. The beam-beam induced loss rate in this mode was $1.1 \times 10^9 \text{ s}^{-1}$ ($\tau_{e^+} = 1.2 \times 10^3 \pm 175 \text{ s}$) without BBLRC, and $0.55 \times 10^9 \text{ s}^{-1}$ ($\tau_{e^+} = 2.0 \times 10^3 \pm 360 \text{ s}$) with BBLRC. Clearly, the application of compensating wires resulted in a two-fold improvement of the beam-beam induced losses for identical beam parameters.

Table 1: DAΦNE machine and beam parameters during 2005-2006 operation with KLOE detector (March, 2006).

Parameter	Value
Number of bunches	105
Bunch spacing	2.7 ns
Full horizontal crossing angle	29 mrad
Number of electrons / bunch	3×10^{10}
Number of positrons / bunch	1×10^{10}
Electron emittance, r.m.s. (x,y)	0.4, 0.0056 μm
Positron emittance, r.m.s. (x,y)	0.4, 0.0012 μm
Momentum spread, r.m.s.	4×10^{-4}
Bunch length, r.m.s. (e^- , e^+)	3.0, 1.1 cm
Electron betatron tunes (x,y)	0.084, 0.157
Positron betatron tunes (x,y)	0.111, 0.191
Damping decrements (x,y,z)	(9, 9, 18.1) $\times 10^{-6}$
Beta-function at IP (x,y)	168, 1.8 cm
Beam-beam parameter, e^+ (x,y)	0.032, 0.029

SIMULATION MODEL

The present version of Lifetrac allows importing the machine optics data for both the weak and the strong beams from MAD-X [16] files. The coordinates of particles in the weak beam are tracked through the accelerator lattice element-by-element, thus allowing for a complete treatment of the lattice nonlinearities, imperfections, strong coupling in the IR due to the detector solenoid, and chromaticity. This is a considerable improvement over the studies performed in 2004-2005, when the machine arcs were represented by linear maps.

An important attribute of Lifetrac is the capability to simulate the macroscopic measurable quantities, which allows for a direct comparison with experiment. For the case of electron-positron colliders, the code computes the equilibrium distribution for weak beam, and evaluates the specific luminosity and beam lifetime provided that the machine aperture is known [14]. We extracted the scraper positions during the experimental runs and incorporated the corresponding aperture restrictions in the modelling. The simulations were performed for the *weak* positron beam, as for the one the most affected by long-range beam-beam interactions. Parameters of the beams in simulation were as listed in Tab. 1.

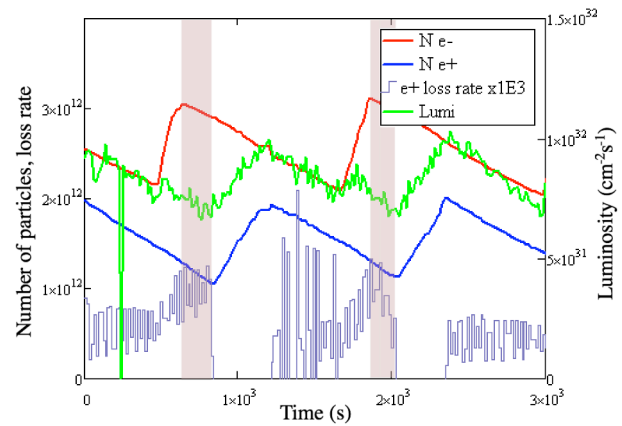


Figure 1: Evolution of beam intensity, beam-beam positron losses ($\times 10^3 \text{ s}^{-1}$) and luminosity without beam-beam compensation.

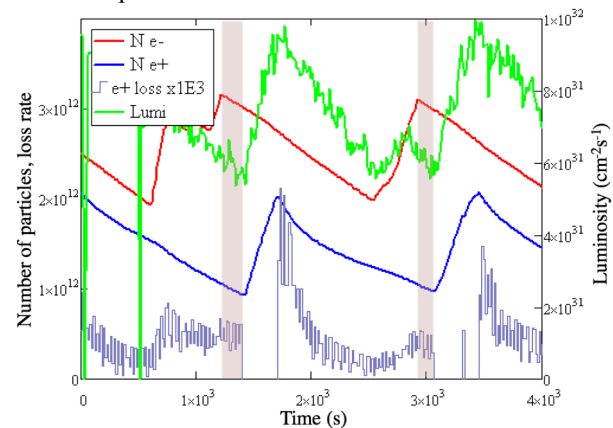


Figure 2: Evolution of beam intensity, beam-beam positron losses ($\times 10^3 \text{ s}^{-1}$) and luminosity with beam-beam compensation.

RESULTS

Figures 3, 4 show the FMA plots for the cases of BBLRC off and on, respectively. The area of complete overlapping of resonant islands, shown in red, represents the boundary of stable motion, the dynamical aperture (DA). It is obvious that the application of BBLRC improves the horizontal DA by some 1σ – from 8 to 9-9.5. The effect is seen for both on- and off-momentum particles. The apparent increase of DA should result in an improvement of the injection efficiency (the beams are injected into DAΦNE in the horizontal plane), and better beam lifetime.

The results of beam density distribution calculations are presented in Figs. 5 and 6. The horizontal scrapers were placed at the distance of 12σ and the vertical aperture was determined by the vacuum pipe dimensions, and corresponded to 100σ beam. These plots show two remarkable features: a) the size of the beam core is the same for BBLRC on and off, and corresponds to a specific luminosity of $2.2 \times 10^{13} \text{ cm}^{-2}$, which is in excellent agreement with the actual luminosity in experiment; and b) the case with wire compensators on exhibits much smaller tail formation. The number of particles transported to large horizontal amplitudes and reaching

the horizontal scrapers is smaller, which reflects in a better beam lifetime.

The results of lifetime calculations are presented in Fig. 7. We performed the calculations for different values of the limiting horizontal aperture in order to determine the dependence of the result on the position of the boundary. The application of BBLRC shows a marked improvement of the beam lifetime – from $2\div 3 \times 10^3$ s without compensation to $\sim 10^5$ s with compensation in a wide range of horizontal apertures. The difference is diminishing at about 8σ , where the tail populations for both cases become somewhat equal. In operation, the scrapers were positioned at $8\text{-}9\sigma$ as reported by the control system read-backs. Together with the lifetime calculation with the code having the accuracy of about 50%, this makes the obtained results to be in a remarkable agreement with experiment.

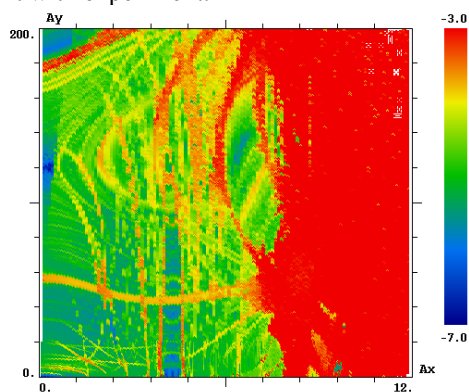


Figure 3: FMA in the space of betatron amplitudes (in units of beam σ) with BBLRC off. Colour depicts the tune jitter in logarithmic scale over the length of tracking (2^{13} turns).

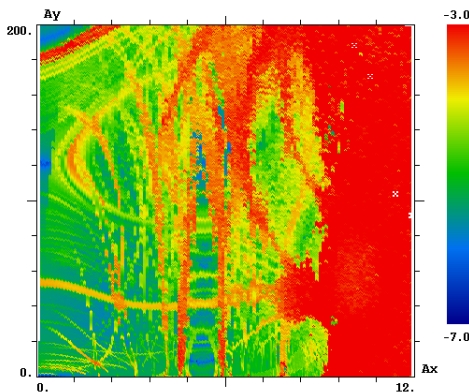


Figure 4: FMA in the space of betatron amplitudes (in units of beam σ) with BBLRC on.

CONCLUSIONS

The experimental data from DAΦNE beam-beam compensation experiment shows a two-fold improvement of the positron beam lifetime due to the compensation at constant specific luminosity. The numerical simulations of beam-beam effects with weak-strong code Lifetrac were used to design the compensation scheme. Modeling with an improved version of the code taking full account of the machine features is in good quantitative agreement

5: Beam Dynamics and EM Fields

with experiment, and reproduce the macroscopic collider performance parameters, such as the specific luminosity and beam lifetime. The achieved level of precision allows to make quality predictions of beam-beam performance of future machines, such as the HL-LHC.

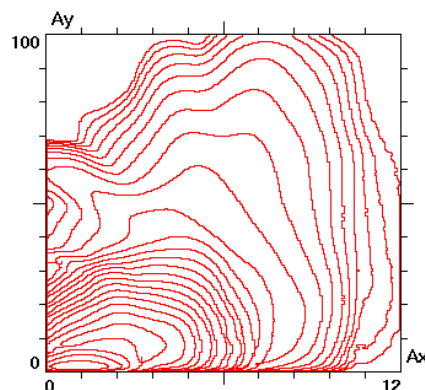


Figure 5: Lines of constant density in the space of betatron amplitudes (in units of beam σ), BBLRC off. Horizontal aperture restriction at 12σ .

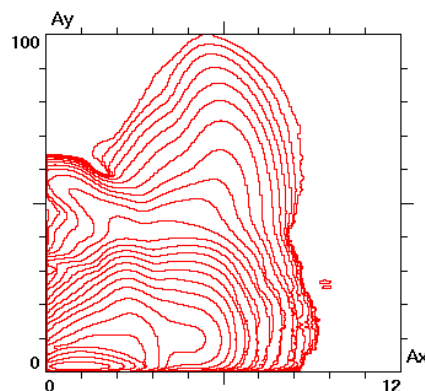


Figure 6: Lines of constant density in the space of betatron amplitudes (in units of beam σ), BBLRC on.

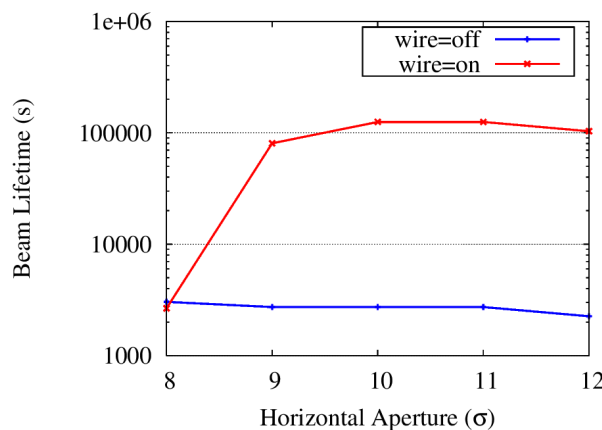


Figure 7: Simulated positron beam lifetime as a function of horizontal aperture restriction.

ACKNOWLEDGMENT

The authors D.S. and A.V. would like to thank the DAΦNE team for hospitality during their visits.

REFERENCES

- [1] V. Shiltsev et al., “Beam-beam effects in the Tevatron”, *Phys. Rev. ST Accel. Beams* **8**, 101001 (2005).
- [2] V. Shiltsev and A. Valishev, “Long-range beam-beam effects in the Tevatron”, ICFA Mini-Workshop on Beam-Beam Effects in Hadron Colliders, CERN, Geneva, Switzerland, 18-22 Mar 2013, pp.101-107 <http://arxiv.org/abs/1410.3653>
- [3] LHC Design Report, CERN-2004-003-V-1 (2004), p.117.
- [4] W. Herr et al., “Long Range Beam-beam Effects in the LHC”, ICFA Mini-Workshop on Beam-Beam Effects in Hadron Colliders, CERN, Geneva, Switzerland, 18-22 Mar 2013, pp.87-92 <http://arxiv.org/abs/1409.4942>
- [5] <https://espace.cern.ch/HiLumi/PLC/default.aspx>
- [6] T. Pieloni and A. Valishev, “HiLumi LHC Deliverable Report: Beam-Beam Effects”, CERN-ACC-2014-0298 (2014).
- [7] J.P. Koutchouk, “Principle of a Correction of the Long-Range Beam-Beam Effect in LHC using Electromagnetic Lenses”, LHC-Project-Note 223, CERN, Geneva, Switzerland, (2000).
- [8] U. Dorda et al., “LHC Beam-Beam Compensation using Wires and Electron Lenses”, Proceedings of PAC07, Albuquerque, NM, USA (2007).
- [9] H.J. Kim et al., “Simulations of beam beam and beam-wire interactions in RHIC”, *Phys. Rev. ST Accel. Beams* **12**, 031001 (2009).
- [10] T. Rijoff et al., “Simulation Studies for the LHC Long-Range Beam-Beam Compensators”, Proceedings of IPAC2012, New Orleans, LA, USA (2012).
- [11] U. Dorda et al., “Wire excitation experiments in the CERN SPS”, Proceedings of EPAC08, Genoa, Italy (2008).
- [12] R. Calaga et al., “Long-range beam-beam experiments in the Relativistic Heavy Ion Collider”, *Phys. Rev. ST Accel. Beams* **14**, 091001 (2011)
- [13] C. Milardi et al., “DAFNE Lifetime Optimization with Compensating Wires and Octupoles”, arXiv:0803.1544, (2008). <http://arxiv.org/abs/0803.1544>
- [14] D. Shatilov, *Particle Accelerators* 52:65-93, (1996).
- [15] D. Shatilov et al., “Application of frequency map analysis to beam-beam effects study in crab waist collision scheme”, *Phys. Rev. ST Accel. Beams* **14**, 014001 (2011).
- [16] <http://cern.ch/madx>